Special Feature: Metallic Materials

Research Report

Effect of Nano-sized Grain Boundary on Coercivity of NdFeB Magnets

Takashi Sato, Tetsu Ohsuna, Yuji Kaneko, Yukiko Takahashi, Kazuhiro Hono and Toshiyuki Shima

Report received on Jul. 20, 2012

ABSTRACT The effects of the nano-grains and the grain boundaries in Nd-Fe-B magnets on the coercivity (H_{cJ}) were investigated through an analysis of the relation between the structure and magnetic properties of ternary Nd-Fe-B thin films. Nd-Fe-B films ranging from 2 to 50 nm in thickness (t) were grown aligned in the (001) direction of the $Nd_2Fe_{14}B$ phase under all conditions. Atomic force microscopy (AFM) revealed that the morphology of the Nd-Fe-B film changed from islands to a continuous thin film with increasing t, based on the Volmer-Webber growth mechanism. This change indicates that magnetic state of the film shifts from single-domain particles to multiple-domain particles with increasing t. The maximum H_{cJ} in as-prepared Nd-Fe-B thin films showed 19.5 kOe at t = 8 nm. From the initial magnetization curve and the AFM image, the film with t = 8 nm was composed of both single-domain particles and multiple-domain particles. In contrast, H_{cJ} of Nd-Fe-B/$Nd_{36}Cu_{64}$ films post-annealed at 400°C was 26.1 kOe. The increase in H_{cJ} results from the suppression of the exchange coupling between $Nd_2Fe_{14}B$ grains separated by the grain boundary, which is enriched by non-magnetic elements of Nd and Cu.

KEYWORDS Coercivity, Nd-Fe-B, Nano-structure, Grain Boundary, Nd-Cu, Thin Film, Sputter, Diffusion, Perpendicular Anisotropy

1. Introduction

Nd-Fe-B magnets[1] are widely used in various applications as a magnetomotive force because these magnets have a large maximum energy product ($(BH)_{max}$ ~60 kOe) and a high saturation magnetization (M_s = 1.6 T)[2]. In particular, a high coercivity of Nd-Fe-B magnets is required in high-temperature environments, such as motors in hybrid vehicles and electric vehicles. However, the coercivity of Nd-Fe-B magnet has been reported to be ~13 kOe (only 20% of the theoretical value[3] estimated by both the magnetocrystalline anisotropy and the saturation magnetization). The coercivity was improved by using (Nd, Dy)-Fe-B alloys partially substituting Dy for Nd because the anisotropy field of the alloys is higher than that of $Nd_2Fe_{14}B$ alloy.[4,5]

The reduction of Dy has been intensively investigated in order to solve the resource problem involving rare earth elements. Dy-diffusion processes in grain boundaries between the Nd-Fe-B grains have attracted much attention.[6-9] On the other hand, studies on the improvement of coercivity without Dy have also focused on the grain boundary.[10-14] For instance, W. F. Li et al. reported that an improvement in coercivity for sintered Nd-Fe-B magnets, including Cu, resulted from the formation of a Cu-rich grain boundary, indicating the suppression of the exchange coupling between neighbor Nd-Fe-B grains. The grain boundary is believed to be a key factor in improving the coercivity. Therefore, a number of studies using a thin film fabrication technique have been conducted in order to control both the microstructure and the boundary of Nd-Fe-B magnets.[15-24]

In the present study, in order to clarify the effect of the nano-grains and the grain boundaries of Nd-Fe-B magnets on the coercivity, ternary Nd-Fe-B thin films were formed by the direct-current (dc) magnetron sputtering method and their structure and magnetic properties were investigated. In particular, post-annealed Nd-Fe-B/Nd-Cu thin films have been successfully fabricated in order to elucidate the above effect.

2. Experimental

Cr/Mo/Nd-Fe-B/Cr thin films and Cr/Mo/Nd-Fe-B/Nd-Cu/Cr multilayered thin films were fabricated on

single-crystal MgO (100) substrates using a UHV-compatible dc magnetron sputtering system with a base pressure of less than 1×10^{-8} Pa. The Ar gas pressure was maintained at 0.13 Pa during deposition. A 1-nm-thick Cr seed layer and a 20-nm-thick Mo buffer layer were epitaxially grown on MgO substrates at room temperature (RT). The substrate temperature was maintained at 625°C during the deposition of the Nd-Fe-B layer. A 10-nm-thick Cr layer was formed as a topmost layer at RT in order to prevent oxidation. $Nd_2Fe_{14}B$ was formed by co-sputtering with Fe, $Fe_{80}B_{20}$, and Nd. Hereinafter, the numerical subscript of alloys denotes atomic percent (at%). The composition of the Nd-Fe-B layer was adjusted to $Nd_{15.2}Fe_{70.2}B_{14.6}$, which was a Nd-rich and B-rich composition compared to that of stoichiometric $Nd_2Fe_{14}B$. The thickness (t) of the Nd-Fe-B film ranged from 2 to 50 nm. Here, t was estimated from the deposition rate of 0.04 nm/s and the deposition time.[25,26] The diffusion of Nd and Cu into the Nd-Fe-B layer was conducted by co-sputtering with both Nd and Cu onto the Nd-Fe-B layer at RT and subsequent annealing at 400 or 500°C for 1 h. Here, thickness of the Nd-Cu layer was 0.5 or 1 nm.[26]

The composition of the films was determined by electron probe x-ray micro-analysis (EPMA). The structural analysis was performed by X-ray diffraction (XRD) with Cu Kα radiation. The surface morphology was observed by atomic force microscopy (AFM) and the microstructure was analyzed by both high-resolution transmission electron microscopy (HRTEM) and scanning transmission electron microscopy (STEM). Energy dispersive X-ray spectroscopy (EDS) revealed the elemental distribution in the film. The magnetization curves were measured with a superconducting quantum interference device (SQUID) magnetometer in the field up to 70 kOe at RT. The magnetic field was applied in the perpendicular direction to the film and in the in-plane direction to confirm the magnetic anisotropy.

3. Results and Discussion

3. 1 Effect of Morphology of Nd-Fe-B on Coercivity[25]

Figure 1 shows XRD patterns for Nd-Fe-B films with t = 2 to 50 nm. The sharp diffraction peaks denoted by the asterisks are due to the MgO (100) substrate, and the peak from the Mo (200) is also observed clearly at around $2\theta = 58.6°$ for all of the films. The peak observed at $2\theta = 65.2°$ is identified as the diffraction from Fe (200) for the film with t = 2 nm. Moreover, the peaks from $Nd_2Fe_{14}B$ (004) and (0010) appeared primarily at 29.3° and 78.3° for all of the films. However, for the films with t = 20 and 50 nm, the peaks from $Nd_{1+\varepsilon}Fe_4B_4$ (200) and Nd (004) began to appear at 25.0° and 30.3°, respectively. The orientation of the film was also confirmed from a cross-sectional TEM image of the film with t = 5 nm, as shown in **Fig. 2**. The c plane of the tetragonal $Nd_2Fe_{14}B$ phase was clearly observed parallel to the film plane. These results indicate that the $Nd_2Fe_{14}B$ phase grows with the (001) orientation.

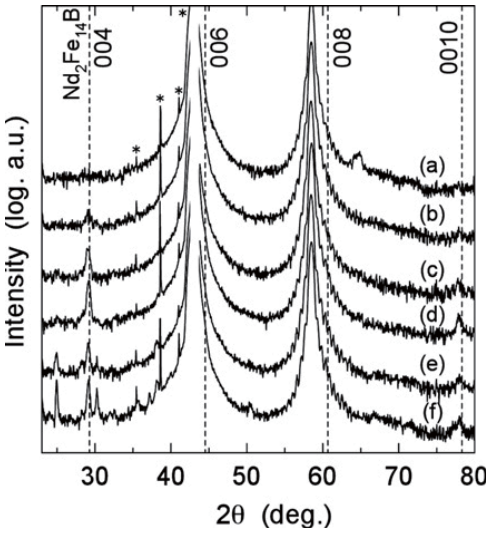

Fig. 1 X-ray diffraction patterns for the Nd-Fe-B films with (a) t = 2 nm, (b) 5 nm, (c) 8 nm, (d) 10 nm, (e) 20 nm, and (f) 50 nm. Asterisks denote the peaks from the MgO (100) single-crystal substrate.

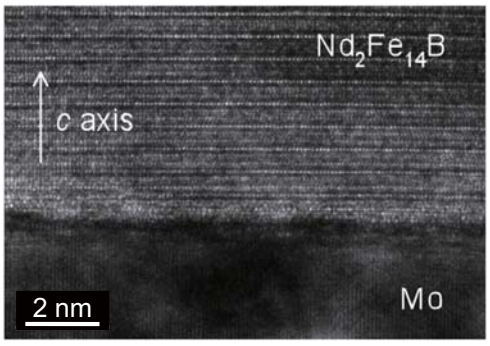

Fig. 2 Cross-sectional TEM image of the Nd-Fe-B film with t = 5 nm.

Figure 3 shows AFM images of the films with different t. The surface morphology changed with t via the Volmer-Webber growth mechanism. Isolated islands, ranging from 20 to 100 nm, appeared and grew for t = 5 to 20 nm. Then, a continuous structure was formed for t > 20 nm.

The magnetization curves for various t are shown in **Fig. 4**. The magnetic easy axis is perpendicular to the film plane and corresponds to the direction of c axis, as shown in Fig. 1. The initial magnetization curves changed with increasing t. In the cases of t = 2 and 5 nm, the initial magnetization curves show a slow start to magnetize and so could not be fully satureated below 20 kOe as an external magnetic field. In contrast, the initial magnetization curves of t = 8, 10, and 20 nm show a steep increase in each initial magnetization curve. The magnetization of the film with t = 50 nm increases steeply and saturates at approximately 10 kOe. The slow increase of the initial magnetization curve with increasing magnetic field indicates the rotation of magnetization by the single-domain particles. On the other hand, the steep increase in magnetization at a low magnetic field is dominated by the domain wall displacement in the multiple-domain particles.[27] The change in the magnetic domain structure indicated by the initial magnetization curves corresponds to the growth of the particles, as shown in the AFM images (Fig. 3). The effect of t for the Nd-Fe-B thin films on the coercivity (H_{cJ}) is shown in **Fig. 5**. With decreasing t, H_{cJ} increased in the films with t > 8 nm due to the change from the multiple-domain particles to the single-domain particles. In contrast, H_{cJ} in the films with t < 8 nm decreased remarkably with decreasing t. This may be attributed to the distortion of the $Nd_2Fe_{14}B$ structure. Here, H_{cJ} of the film showed a maximum value of 19.5 kOe at t = 8 nm, and the domain structure of the film consisted of a mixture of single-domain and multiple-domain particles.

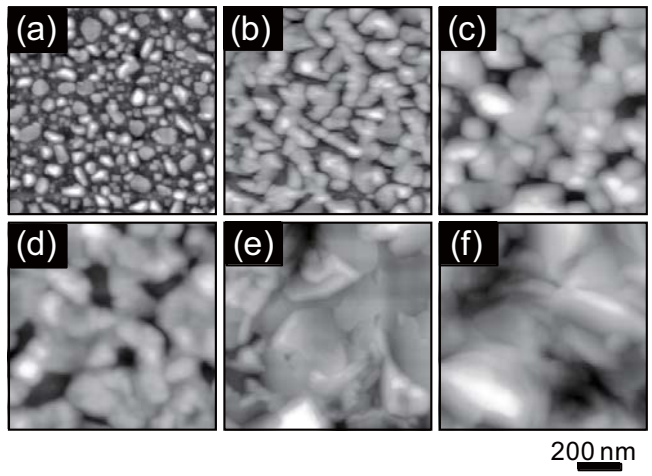

Fig. 3 Atomic force microscopy images of the Nd-Fe-B films with various film thicknesses ((a) t = 2 nm, (b) 5 nm, (c) 8 nm, (d) 10 nm, (e) 20 nm, and (f) 50 nm).

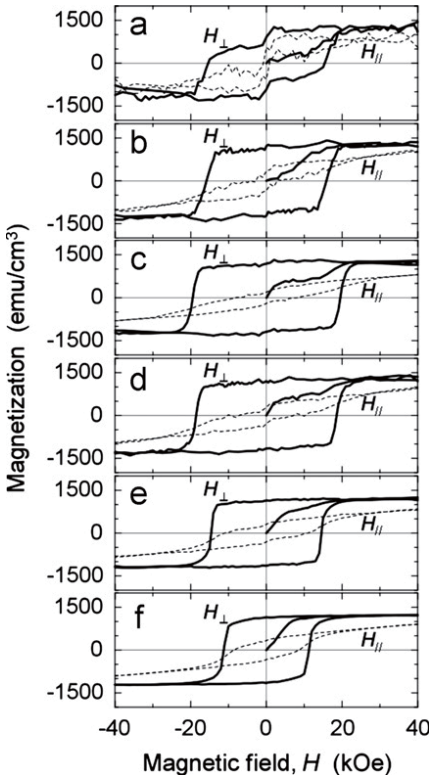

Fig. 4 Magnetization curves for the Nd-Fe-B films with various film thicknesses ((a) t = 2 nm, (b) 5 nm, (c) 8 nm, (d) 10 nm, (e) 20 nm, and (f) 50 nm; solid lines: $H \perp$ film plane, dashed lines: H // film plane).

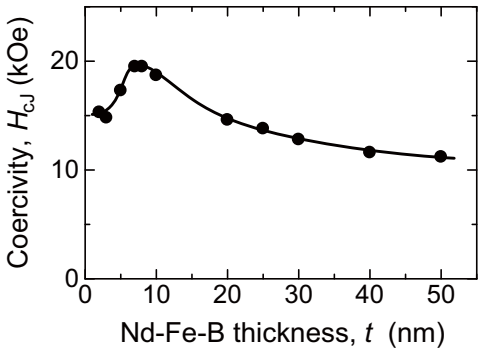

Fig. 5 Coercivity of the Nd-Fe-B thin film as a function of film thickness t.

3. 2 Effect of Grain Boundary on Coercivity[26]

The magnetization curves of Nd-Fe-B (30 nm)/ Nd-Cu (1 nm) thin films with different Cu concentrations x in the $Nd_{100-x}Cu_x$ layer are shown in **Fig. 6**, where x = 0, 18, 64, 78, and 100. These films were post-annealed at 500 °C for 1 h. As a reference, an Nd-Fe-B film without post-annealing was prepared, and the curves are shown in Fig. 6(f). The magnetic field of 45 kOe was not sufficient to saturate the magnetization in the in-plane direction, indicating the existence of a large perpendicular magnetic anisotropy. Here, H_{cJ} of 12.8 kOe was obtained for the film without post-annealing, and a steep increase in the initial magnetization curve below 7 kOe was observed. In contrast, a remarkable increase in H_{cJ} for the annealed specimen was observed, while the initial magnetization curve is similar. However, a large magnetic field was needed in order to saturate the magnetization. Here, H_{cJ} of the annealed film with the Nd layer (x = 0) increased slightly compared to that of the as-prepared Nd-Fe-B film. With increasing x in the $Nd_{100-x}Cu_x$ layer, H_{cJ} increased and exhibited a large value of 23 kOe at x = 64. H_{cJ} was drastically improved at $Nd_{36}Cu_{64}$ (at.%), even though the composition is far from that of the Nd-Cu eutectic alloy ($Nd_{70}Cu_{30}$). This may be associated with the effect of ternary or more complex compositions for the decrease in the solidification temperature. Eventually, the simultaneous diffusion of Nd and Cu elements into the Nd-Fe-B layer is effective in improving H_{cJ}.

The effect of post-annealing on H_{cJ} for Nd-Fe-B and Nd-Fe-B/ $Nd_{36}Cu_{64}$ thin films is presented in **Fig. 7** as a function of t. The post-annealing temperature was 400°C. The thickness of the $Nd_{36}Cu_{64}$ layer was 0.5 nm. With increasing t, H_{cJ} increased and showed a maximum value of 19.5 kOe at t = 8 nm for the as-prepared film without annealing, and H_{cJ} of the post-annealed film exhibited a similar tendency. In contrast, H_{cJ} of the post-annealed Nd-Fe-B/$Nd_{36}Cu_{64}$ film exhibited extreme increases of approximately 5 kOe at every thickness. The film with the highest value of 26.1 kOe was obtained at t = 8 nm.

In order to clarify the effect of the Nd-Cu alloy cap layer on the Nd-Fe-B thin films with post-annealing on the improvement of H_{cJ}, structural analysis and microstructural observation were performed. **Figure 8** shows a cross-sectional HRTEM image of the Nd-Fe-B (30 nm)/$Nd_{36}Cu_{64}$ (0.5 nm) film with post-annealing. Three grains and their grain boundaries are evident in this figure. In the grain boundaries

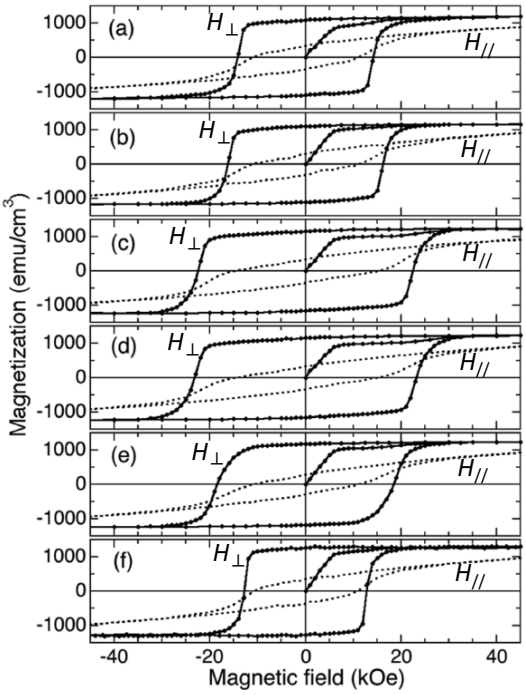

Fig. 6 Magnetization curves of Nd-Fe-B (30 nm)/Nd-Cu (1 nm) thin films with different Cu concentrations x in the Nd_{100-x} Cux layer, where x are (a) 0, (b) 18, (c) 64, (d) 78, and (e) 100 at.%. These films were post-annealed at 500°C for 1 h. As a reference, the curves of the as-deposited Nd-Fe-B film without Nd-Cu are also presented in (f). Solid lines: $H \perp$ film plane, dashed lines: H // film plane.

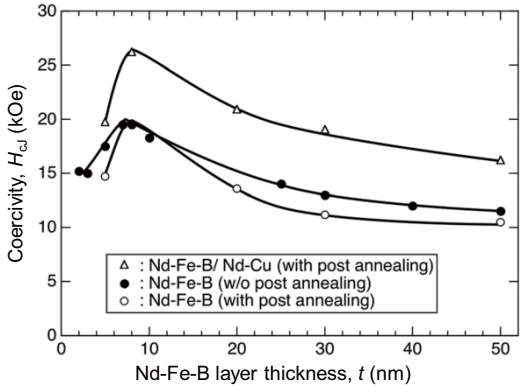

Fig. 7 Effect of post-annealing on H_{cJ} for Nd-Fe-B and Nd-Fe-B/$Nd_{36}Cu_{64}$ thin films as a function of t. The thickness of the $Nd_{36}Cu_{64}$ layer was 0.5 nm. The post-annealing temperature was 400°C. The symbols represent Nd-Fe-films with (open circles) and without (closed circles) post-annealing, and Nd-Fe-B/$Nd_{36}Cu_{64}$ films with post-annealing (open triangles).

between these grains, an amorphous structure with a thickness of approximately 1 nm was confirmed. The cross-sectional dark-field STEM image and EDS maps of each element for Nd-Fe-B (30 nm)/$Nd_{36}Cu_{64}$ (1 nm) film before post-annealing are shown in **Fig. 9**. The Mo buffer layer, the Nd-Fe-B layer, and the Cr oxidation protection layer were observed in the STEM image. From the EDS maps, intense signals from Cr, Mo, and Cu were clearly detected at each layer. The Nd and Fe elements in the Nd-Fe-B layer showed a wide distribution in the Nd-Fe-B layer. The bright and dark contrasts in the Fe map correspond to the formation of the $Nd_2Fe_{14}B$ and $Nd_{1+\varepsilon}Fe_4B_4$ phases, as shown in Fig. 1.

For the Nd-Fe-B (30 nm)/$Nd_{36}Cu_{64}$ (0.5 nm) film after post-annealing at 400°C for 1 h, the cross-sectional dark field STEM image and EDS maps of each element are shown in **Fig. 10**. Intense signals from a Mo buffer layer and a Cr protection layer were detected at the bottom and the top, respectively, of the Nd-Fe-B layer. On the other hand, the Cu element disappeared from the top of the layer after post-annealing, but appeared in the grain boundary between the $Nd_2Fe_{14}B$ grains. On the grain boundary, the Nd element was slightly concentrated, and the Fe element was remarkably reduced. The reduction in the Fe concentration in the grain boundary of Nd-Fe-B grains provides a magnetically-decoupling of the Nd-Fe-B grains, which suppresses the domain wall motion in the magnetization reversal process. This result is in agreement with studies on the coercivity enhancement of nano-sized Nd-Fe-B powders by the diffusion of Nd-Cu[28] or Nd-Cu-Al[29] alloy. Therefore, the infiltration of non-magnetic elements into the grain boundary is an effective way to improve H_{cJ} because of the suppression of the exchange coupling between $Nd_2Fe_{14}B$ grains.

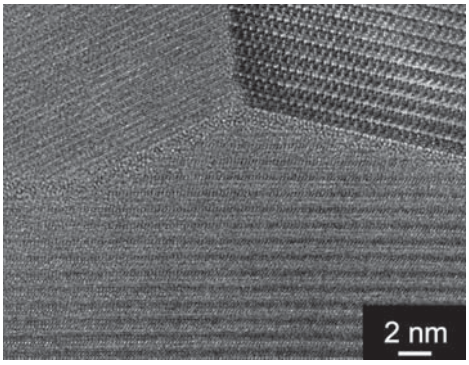

Fig. 8 Cross-sectional HRTEM image of the Nd-Fe-B (30 nm)/$Nd_{36}Cu_{64}$ (0.5 nm) film post-annealed at 400°C.

4. Conclusion

In order to clarify the effect of the nano-grains and the grain boundaries of Nd-Fe-B magnets on the coercivity, ternary Nd-Fe-B thin films were formed by the direct-current (dc) magnetron sputtering method, and their structure and magnetic properties were investigated. The morphology of the films changed

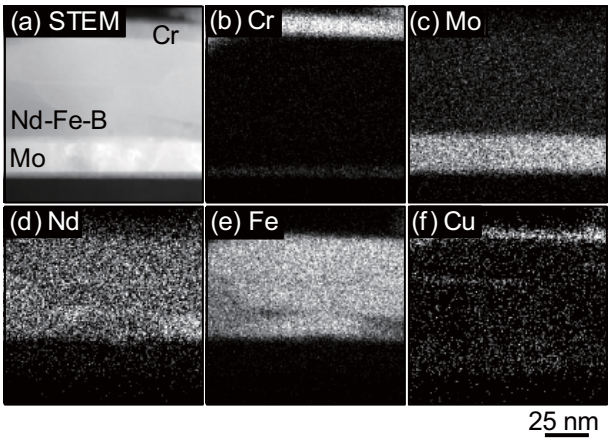

Fig. 9 (a) Cross-sectional dark field STEM image and EDS elemental maps of (b) Cr-Kα, (c) Mo-Kα, (d) Nd-Lα, (e) Fe-Kα, and (f) Cu-Kα for the Nd-Fe-B (30 nm)/$Nd_{36}Cu_{64}$ (1.0 nm) film before post-annealing.

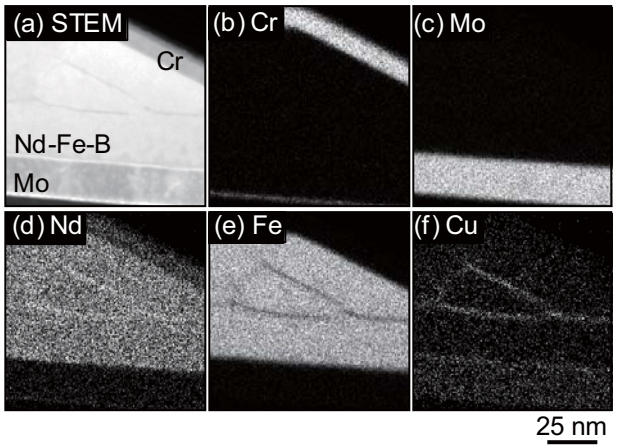

Fig. 10 (a) Cross-sectional dark-field STEM image and EDS elemental maps of (b) Cr-Kα, (c) Mo-Kα, (d) Nd-Lα, (e) Fe-Kα, and (f) Cu-Kα for the Nd-Fe-B (30 nm)/$Nd_{36}Cu_{64}$ (0.5 nm) film after post-annealing at 400°C.

from an island structure to a continuous structure with increasing thickness (t), indicating that the magnetic state of the films shifted from single-domain particles to multi-domain particles with increasing t. The maximum coercivity (H_{cJ}) of the Nd-Fe-B thin films was 19.5 kOe at t = 8 nm, where the films were composed of both single-domain and multiple-domain particles from the initial magnetization curve.[25] When the effect of the infiltration of Nd-Cu into the Nd-Fe-B layer on the coercivity was investigated, H_{cJ} showed a remarkable enhancement from 19.5 kOe to 26.1 kOe for the Nd-Fe-B (8 nm)/$Nd_{36}Cu_{64}$ (0.5 nm) films after the optimum post-annealing. Nd and Cu enrichment was clearly observed at the grain boundary of the $Nd_2Fe_{14}B$ grains, whereas the concentration of Fe in the grain boundary phase decreased. This structural change, which suppresses the exchange coupling between $Nd_2Fe_{14}B$ grains, provides the increase in H_{cJ}. These results suggest that controlling the nano-sized grain boundary through the infiltration of non-magnetic elements of Nd and Cu is extremely effective for improving the coercivity of Nd-Fe-B magnets.[26]

Acknowledgements

We would like to thank our collaborators and coauthors, including N. Oka and S. Suzuki (Tohoku-Gakuin University). The present study was a collaboration with H. Kato (TOYOTA CRDL, INC.) and was supported in part by Toyota Motor Corporation. We would also like to thank the Hi-tech Research Center of Tohoku-Gakuin University for their experimental support. Finally, we would like to thank Elsevier Ltd. and the American Institute of Physics for permission to reproduce this paper.

Reference

(1) Sagawa, M., Togawa, N., Yamamoto, H. and Matsuura, Y., "New Material for Permanent Magnets on a Base of Nd and Fe (invited)", *J. Appl. Phys.*, Vol.55, No.6 (1984), p.2083.

(2) Hirosawa, S., Matsuura, Y., Yamamoto, H., Fujimura, S., Sagawa, M. and Yamauchi, H., "Magnetization and Magnetic Anisotropy of $R_2Fe_{14}B$ Measured on Single Crystals", *J. Appl. Phys.*, Vol.59, No.3 (1986), p.873.

(3) Kronmüllur, H., "Theory of Nucleation Fields in Inhomogeneous Ferromagnets", *Phys. Status Solidi* (*b*), Vol.144, No.1 (1987), p.385.

(4) Burzo, E., "Permanent Magnets Based on R-Fe-B and R-Fe-C alloys", *Rep. Prog. Phys.*, Vol.61, No.9 (1998), p.1099.

(5) Bai, G., Gao, R. W., Sun, Y., Han, G. B. and Wang, B., "Study of High-coercivity Sintered NdFeB Magnets", *J. Magn. Magn. Mater.*, Vol.308, No.1 (2007), p.20.

(6) Park, K. T., Hiraga, K. and Sagawa, M., "Effect of Metal-coating and Consecutive Heat Treatment on Coercivity of Thin Nd-Fe-B Sintered Magnets", *Proceedings 16th International Workshop on Rare-Earth Magnets and Their Applications* (2000), pp.257-264, The Japan Institute of Metals.

(7) Nakamura, H., Hirota, K., Shimano, M., Minowa, T. and Honshima, M., "Magnetic Properties of Extremely Small Nd-Fe-B Sintered Magnets", *IEEE Trans. Magn.*, Vol.41, No.10 (2005), p.3844.

(8) Suzuki, H., Satsu, Y. and Komuro, M., "Magnetic Properties of a Nd-Fe-B Sintered Magnet with Dy Segregation", *J. Appl. Phys.*, Vol.105, No.7 (2009), 07A734.

(9) Li, W. F., Sepehri-Amin, H., Ohkubo, T., Hase, N. and Hono, K., "Distribution of Dy in High-coercivity (Nd,Dy)-Fe-B Sintered Magnets", *Acta Materialia*, Vol.59 (2011), p.3061.

(10) Shinba, Y., Konno, T. J., Ishikawa, K., Hiraga, K. and Sagawa, M., "Transmission Electron Microscopy Study on Nd-rich Phase and Grain Boundary Structure of Nd-Fe-B Sintered Magnets", *J. Appl. Phys.*, Vol.97, No.5 (2005), 053504.

(11) Li, W. F., Ohkubo, T., Hono, K., Nishiuchi, T. and Hirosawa, S., "The Role of Grain Boundaries in the Coercivity of Hydrogenation Disproportionation Desorption Recombination Processed Nd-Fe-B Powders", *J. Appl. Phys.*, Vol.105, No.7 (2009), 07A706.

(12) Li, W. F., Ohkubo, T. and Hono, K., "Effect of Post-sinter Annealing on the Coercivity and Microstructure of Nd-Fe-B Permanent Magnets", *Acta Mater.*, Vol.57, No.5 (2009), p.1337.

(13) Li, W. F., Ohkubo, T., Hono, K. and Sagawa, M., "The Origin of Coercivity Decrease in Fine Grained Nd-Fe-B Sintered Magnets", *J. Magn. Magn. Mater.*, Vol.321, No.8 (2009), p.1100.

(14) Sepehri-Amin, H., Li, W. F., Ohkubo, T., Nishiuchi, T., Hirosawa, S. and Hono, K., "Effect of Ga addition on the Microstructure and Magnetic Properties of Hydrogenation-disproportionation- desorption-recombination Processed Nd-Fe-B Powder", *Acta Mater.*, Vol.58 (2010), p.1309.

(15) Cadieu, F. J., Cheung, T. D. and Wickramasekara, L., "Magnetic Properties of Sputtered Nd-Fe-B Films", *J. Magn. Magn. Mater.*, Vol.54-57, No.1 (1986), p.535.

(16) Yamashita, S., Yamasaki, J., Ikeda, M. and Iwabuchi, N., "Anisotropic Nd-Fe-B Thin-film Magnets for Milli-size Motor", *J. Appl. Phys.*, Vol.70, No.10 (1991), p.6627.

(17) Kapitanov, B. A., Komilov, N. V., Linetsky, Y. L. and Tsvekov, V. Y., "Sputtered Permanent Nd-Fe-B

Magnets", *J. Magn. Magn. Mater.*, Vol.127, No.3 (1993), p.289.
(18) Lemke, H., Lang, T., Goddenhenrich, T. and Heiden, C., "Micro Patterning of Thin Nd-Fe-B Films", *J. Magn. Magn. Mater.*, Vol.148, No.3 (1995) p.426.
(19) Parhofer, S., Kuhrt, C., Wecker, J., Gieres, G. and Schultz, L., "Magnetic Properties and Growth Texture of High-coercive Nd-Fe-B Thin Films", *J. Appl. Phys.*, Vol.83, No.5 (1998), p.2735.
(20) Shima, T., Kamegawa, A., Hono, K. and Fujimori, H., "Overlayer-induced Anisotropic Alignment of $Nd_2Fe_{14}B$ Nanograins", *Appl. Phys. Lett.*, Vol.78, No.14 (2001), p.2049.
(21) Neu, V., Melcher, S., Hannemann, U., Fähler, S. and Schultz, L., "Growth, Microstructure, and Magnetic Properties of Highly Textured and Highly Coercive Nd-Fe-B Films", *Phys. Rev. B*, Vol.70, No.14 (2004), p.144418.
(22) Chen, S. L., Liu, W., Chen, C. L. and Zhang, Z. D., "Effect of Heat Treatment on Microstructure and Magnetic Properties of Anisotropic Nd-Fe-B Films with Mo or Ti Buffer Layer", *J. Appl. Phys.*, Vol.98, No.11 (2005), 113905.
(23) Liu, X., Shiozaki, Y. and Morisako, A., "Magnetization Reversal Mechanism of Ultra Thin $Nd_2Fe_{14}B$ Films with Perpendicular Magnetic Anisotropy", *J. Appl. Phys.*, Vol.103, No.7 (2008), 07E104.
(24) You, C. Y., Takahashi, Y. K. and Hono, K., "Fabrication and Characterization of Highly Textured Nd-Fe-B Thin Film with a Nanosized Columnar Grain Structure", *J. Appl. Phys.*, Vol.108, No.4 (2010), 043901.
(25) Sato, T., Kato, H., Shima. T., Takahashi, Y. K. and Hono, K., "Effect of Film Morphology on the Magnetic Properties for Nd-Fe-B Thin Films", *J. Magn. Magn. Mater.*, Vol.323, No.1 (2011), p.162.
(26) Sato. T., Oka. N., Ohsuna, T., Kaneko, Y., Suzuki, S. and Shima. T., "Enhancement of Coercivity for Nd-Fe-B Thin Films by the Inflation of Nd-Cu Alloy Cap Layer", *J. Appl. Phys.*, Vol.110, No.2 (2011), 023903.
(27) Shima, T., Takanashi, K., Takahashi, Y. K. and Hono, K., "Preparation and Magnetic Properties of Highly Coercive FePt Films", *Appl. Phys. Lett.*, Vol.81, No.6 (2002), p.1050.
(28) Sepehri-Amin, H, Ohkubo, T., Nishiuchi, T., Hirosawac, S. and Honoa, K., "Coercivity Enhancement of Hydrogenation-disproportionation-desorption-recombination Processed Nd-Fe-B Powders by the Diffusion of Nd-Cu Eutectic Aloys", *Scripta Materialia*, Vol.63 (2010), p.1124.
(29) Mishima, C., Noguchi, K., Yamazaki, M., Doi, H., Mitarai, H. and Honkura, Y., "Development of Dy-free Nd-Fe-B Anisotropic Bonded Magnet with High Thermal Stability", *Digests of the 34th Annual Conference on Magnetics in Japan* (2010), p.135, The Magnetics Society of Japan.

Figs. 1-5
Reprinted from J. Magn. Magn. Mater., Vol.323 (2011), pp.163-166, Sato, T., Kato, H., Shima, T., Takahashi, Y. K. and Hono, K., Effect of Film Morphology on the Magnetic Properties for Nd-Fe-B Thin Films, © 2011 Elsevier, with permission from Elsevier.

Figs. 6-10
Reprinted from J. Appl. Phys., Vol.110, (2011), 023903, Sato, T., Oka, N., Ohsuna, T., Kaneko, Y., Suzuki, S. and Shima, T., Enhancement of Coercivity for Nd-Fe-B Thin Films by the Infiltration of Nd-Cu Alloy Cap Layer, © 2011 AIP, with permission from American Institute of Physics.

Takashi Sato
Research Fields:
- Hard Magnet
- Magnetic Thin Film

Academic Degree: Dr.Eng.
Academic Societies:
- The Magnetic Society of Japan
- The Japan Society of Applied Physics

Tetsu Ohsuna
Research Field:
- Electron Microscopy

Academic Degree: Dr.Eng.
Academic Societies:
- The Japan Institute of Metals
- The Japanese Society of Microscopy
- Japan Association of Zeolite

Yuji Kaneko
Research Field:
- Hard Magnet

Academic Degree: Dr.Eng.
Academic Societies:
- Japan Society of Powder and Powder Metallurgy
- The Japan Institute of Metals

Awards:
- The Japan Institute of Metals Technical Development Award, 1998
- Japan Society of Powder and Powder Metallurgy Award, 1998

Yukiko Takahashi*

Research Fields:
- Magnetic Thin Film
- Spintronics
- Transmission Electron Microscope

Academic Degree: Dr.Eng.

Academic Societies:
- The Magnetics Society of Japan
- The Japan Institute of Metals
- The Japan Society of Applied Physics

Awards:
- Oral Presentation Award, The Magnetic Society of Japan, 2004
- The Japan Institute of Metals Micrograph Award, 2005
- The Japan Institute of Metals Young Researcher Award (Materials Physics), 2006

Kazuhiro Hono*

Research Fields:
- Magnetic Material
- Spintronics
- Atom Probe Field Ion Microscope
- Transmission Electron Microscope
- Phase Transformations in Solids

Academic Degree: Ph.D.

Academic Societies:
- The Magnetics Society of Japan
- The Japan Institute of Metals
- IEEE Magnetic Society
- TMS

Awards:
- Light Metal Encouragement Prize, The Japan Institute of Light Metals, 1991
- The Japan Institute of Metals Young Researcher Award, 1992
- The Japan Institute of Metals Meritorious Award, 1997
- Light Metal Advancement Award, The Japan Institute of Light Metals, 2003
- MSJ Outstanding Research Award, 2008
- TMS Fellows Award, 2011
- The Japan Institute of Metals Distinguished Contribution Award, 2011

Toshiyuki Shima**

Research Fields:
- Magnetic Material
- Thin Film

Academic Degree: Dr.Eng.

Academic Societies:
- The Magnetic Society of Japan
- The Japan Institute of Metals
- The Institute of Electrical Engineers of Japan
- IEEE
- Materials Research Society

*National Institute for Materials Science
**Tohoku Gakuin University

